RSC Advances

PAPER

View Article Online
View Journal | View Issue

Open Access Article. Published on 22 June 2022. Downloaded on 1/13/2026 5:05:27 AM.
This article is licensed under a Creative Commons Attribution-NonCommercial 3.0 Unported Licence.

Check for updates

Cite this: *RSC Adv.*, 2022, **12**, 18397

A novel fluorescent digitonin derivative for non-invasive skin cholesterol detection: potential application in atherosclerosis screening†

Jingshu Ni,[ab] Yong Liu,[abc] Haiou Hong,[d] Xiangyong Kong,[d] Yongsheng Han,[d] Lei Zhang,[e] Yang Zhang,[ab] Yuanzhi Zhang,[ac] Changyi Hua,[a] Quanfu Wang,[a] Xia Wang,[a] Yao Huang,[ac] Wang YiKun*[ac] and Dong Meili *[ac]

Received 28th March 2022
Accepted 27th May 2022

DOI: 10.1039/d2ra01982e

rsc.li/rsc-advances

There is a great demand for the rapid and non-invasive atherosclerosis screening method. Cholesterol content in the epidermis of the skin is an early biomarker for atherosclerosis. Risk assessment of atherosclerosis can be achieved by measuring cholesterol in the epidermis. Here, we synthesised a new fluorescent digitonin derivative (FDD) for the non-invasive detection of skin cholesterol. The results of fluorescence spectroscopy studies indicated that the probe exhibited desirable selectivity for cholesterol. The proof-of-concept preclinical study confirmed that FDD can detect different concentrations of skin cholesterol; patients diagnosed with atherosclerotic cardiovascular disease and the at-risk atherosclerosis group exhibited higher skin cholesterol content than the normal group. The area under the ROC curve for distinguishing the normal/disease group was 0.9228 (95% confidence interval, 0.8938 to 0.9518), and the area under the ROC curve for distinguishing the normal/risk group was 0.9422 (95% confidence interval, 0.9178 to 0.9665). We anticipate that this non-invasive skin cholesterol test may be used as a risk assessment tool for atherosclerosis screening in a large population for further examination and intervention in high-risk populations.

1. Introduction

Skin is considered the largest organ in the human body and also the body's first physiological barrier.[1,2] As an important structural component of the skin barrier, lipids have an irreplaceable function in the maintenance of the permeability barrier function of the skin and they also play an antimicrobial role in the skin's immune defence system.[3,4] Cholesterol is one of the major skin barrier lipids; about 30% of the cholesterol in the human body is synthesized in the skin, and 10% to 15% of cholesterol is metabolized through the skin.[5] A study has reported that the physiological level of cholesterol in the stratum corneum (SC) appears to exceed its miscibility with other barrier lipids, and a 0.4 : 1 : 1 M ratio of Chol/ceramides/fatty acids appears sufficient for skin lipids to limit water loss and prevent the entry of environmental substances; the stratum corneum cholesterol may have roles in the skin other than barrier function.[6]

In 1974, Bouissou *et al.* first reported that skin and aortic walls undergo very similar morphological changes with age and atherosclerosis formation, and an increased degree of atherosclerosis is coupled with an increased skin cholesterol.[7] Girardet *et al.* found increased skin cholesterol levels in patients with coronary atherosclerosis. The cholesterol content in the epidermis of the patients with atherosclerosis is closely related to the cholesterol deposited in the arterial wall, and the cholesterol content of the epidermis increases with the degree of atherosclerosis.[8] Subsequently, Melicosilvestre *et al.* and De Graeve *et al.* further demonstrated by skin biopsy that the skin cholesterol content of atherosclerosis patients was about 1.5 times that of normal people.[9] All the previous research was performed by skin biopsy combined with extraction technology, then measured using metrology or liquid chromatography, however, the measuring process is complicated and time-consuming, in 2001, a simple, non-invasive procedure for estimating skin cholesterol, the "three drops" test, was proposed as an alternative screening method.[10] The test, which uses three different concentrations of a digitonin–copolymer–horseradish peroxidase (HRP) conjugate and visual scoring, is capable of

[a]*Anhui Provincial Engineering Technology Research Center for Biomedical Optical Instrument, Anhui Provincial Engineering Laboratory for Medical Optical Diagnosis &Treatment Technology and Instrument, Anhui Institute of Optics and Fine Mechanics, Hefei Institutes of Physical Science, Chinese Academy of Sciences, Hefei, 230031, China. E-mail: dongmeili@aiofm.ac.cn; wyk@aiofm.ac.cn*

[b]*University of Science and Technology of China, Hefei, 230026, China*

[c]*Wanjiang Center for Development of Emerging Industrial Technology, Tongling, 244000, China*

[d]*The First Affiliated Hospital of USTC, Division of Life Sciences and Medicine, University of Science and Technology of China, Hefei, 230001, China*

[e]*Anhui Provincial Institute for Food and Drug Control, Hefei, 230051, China*

† Electronic supplementary information (ESI) available. See https://doi.org/10.1039/d2ra01982e

Open Access Article. Published on 22 June 2022. Downloaded on 1/13/2026 5:05:27 AM.
This article is licensed under a Creative Commons Attribution-NonCommercial 3.0 Unported Licence.

discriminating between healthy individuals, those at risk of developing atherosclerosis, and those with overt disease.[11] The "three drops" test uses quantitative interpretation and a single concentration of detector. The hypothenar eminence of each hand was cleansed with alcohol and allowed to dry. In a die-cut well foam template affixed to the palm, a drop of solution containing a synthetic digitonin-copolymer-horseradish peroxidase conjugate was applied to the prepared area and incubated for 1 minute. The area was blotted and an indicator solution containing a horseradish peroxidase substrate that induces a blue change was applied to the well. Positive and negative control well samples were applied concurrently on the same skin surface. Skin cholesterol levels were quantified based on colour change. Hue development was measured by reflectance using a handheld spectrophotometer, which was interfaced with a computer, and the resulting change in hue was numerically reported in units (U). Skin cholesterol is proved to be associated with angiographic coronary artery disease[12,13] and the presence of myocardial ischemia in patients with positive stress test results using this technique.[10] In asymptomatic patients, there is an association between skin cholesterol, coronary artery calcium, circulating inflammatory markers and carotid intima-media thickness.[14–16] Nevertheless, the synthetic methods of digitonin-copolymer-horseradish are complicated and quality control is difficult. Horseradish peroxidase is an enzyme. After the detection reagent binds to the skin cholesterol, the indicator reagent must be added for a second reaction. The whole test process takes about five minutes to obtain the results but the measured results are easily affected by temperature, pH, and other environmental factors.

In view of the above deficiencies, we have synthesized fluorescent digitonin derivatives (FDD), including a digitonin part that binds specifically to skin cholesterol, a long hydrophilic chain that improves the hydrophilicity, and a fluorescent group that can be excited by a specific wavelength of light. The selectivity of digitonin for cholesterol has been proven by various methods.[17–20] The principle of skin cholesterol detection by FDD is shown in Scheme 1. In short, we excited the skin with 405 nm excitation light before incubating with the FDD. The skin will display a background fluorescence that is generated by the excitation of intrinsic fluorescent substances such as nicotinamide adenine dinucleotide (NADH), flavine adenine dinucleotide (FAD), and advanced glycation end products (AGEs) in the skin. After incubation with FDD, the FDD will selectively bind to the cholesterol. When we stimulated the skin at the incubation site again with 405 nm excitation light, we observed a strong fluorescence enhancement, which was the superposition of the skin background fluorescence and FDD fluorescence combined with cholesterol. When the skin background fluorescence is deducted, the remaining fluorescence is that of FDD combined with cholesterol, and the cholesterol content can be determined from the fluorescence intensity. The remainder of this paper describes the synthesis and characterisation of FDD and proves the accuracy and reliability of the derivatives as well as explores the initial pre-clinical application in atherosclerosis screening.

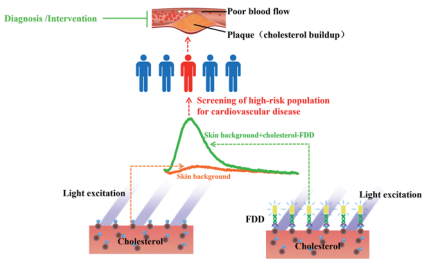

Scheme 1 The principle of skin cholesterol detection by FDD and application in atherosclerotic cardiovascular disease risk screening. FDD can specifically bind to skin cholesterol. The reagent was combined with a fluorescent group. The amount of binding reagent on the skin surface is positively correlated with the content of cholesterol. After combining with skin cholesterol, the test site is irradiated with excitation light with a specific wavelength, and the fluorescence spectrum can provide information about the skin cholesterol content. Skin cholesterol as measured by FDD can be used as part of the risk assessment for atherosclerotic cardiovascular disease where further diagnostic evaluation is being considered. Test results, when considered in conjunction with clinical evaluation, will aid the physician in focusing on diagnostic and patient management options.

2. Results and discussion

2.1 Probe design and synthesis

The main purpose of designing the FDD is to realise the non-invasive detection of cholesterol in the epidermis. The synthetic route is shown in Scheme 2. Digitonin was chosen as the cholesterol recognition unit for its strong interactions with cholesterol, 7-(diethylamino)-2-oxy-2-hydro-benzofuran-3-carboxylic acid was used as the fluor group because its excitation wavelength is greater than 400 nm, which is safe for irradiating the human skin. We chose 2-(2-(2-(2-azoethoxy)ethoxy) ethoxy) ethylamine as the linking arm because its amino group can combine with the carboxyl group of the fluorescent group to improve the water solubility of the fluorescent probe. Purification of digitonin is required before initiating the synthesis of probes. Here, 1 g of the purchased digitonin was dissolved in 20 mL of pure ethanol at 80 °C, then the solution was cooled in ice water at 0 °C for 20 min, and the precipitated digitonin was centrifuged at 4 °C. After repeating the above two steps twice, the resulting precipitate was vacuum dried to obtain purified digitonin.

The skin cholesterol probe was synthesised according to the route shown in Scheme 2 through three steps. First, purified digitonin powder (compound **1**, 620 mg, 0.5 mmol), $Cu(CH_3CN)_4BF_4$ (8 mg, 0.025 mmol), (*S*,*S*)-L (13 mg, 0.05 mmol), 2-oxa-9-boratricyclo[8.4.0.03,]tetradeca-1(14),3,5,7,10,12-hexaen-9-ol (31 mg, 0.15 mmol), and 4 Å molecular sieves (400 mg) were added to a two-necked reaction flask protected by N_2. Carbonic acid, 1,1-dimethylethyl 1-phenyl-2-propyn-1-yl ester (compound **2**, 146 mg, 0.6 mmol), Et_3N (101 mg, 1 mmol) and THF (4 mL) were then added *via* a syringe, with stirring at room temperature for 9 h. After the reaction was completed, the reaction liquid was filtered and washed three times with 2 mL THF. The solvent was evaporated under reduced pressure and then 20 mL of solvent (petroleum ether/ethyl acetate, 10 : 1, v/v) was added to

 © 2022 The Author(s). Published by the Royal Society of Chemistry

Open Access Article. Published on 22 June 2022. Downloaded on 1/13/2026 5:05:27 AM.
This article is licensed under a Creative Commons Attribution-NonCommercial 3.0 Unported Licence.

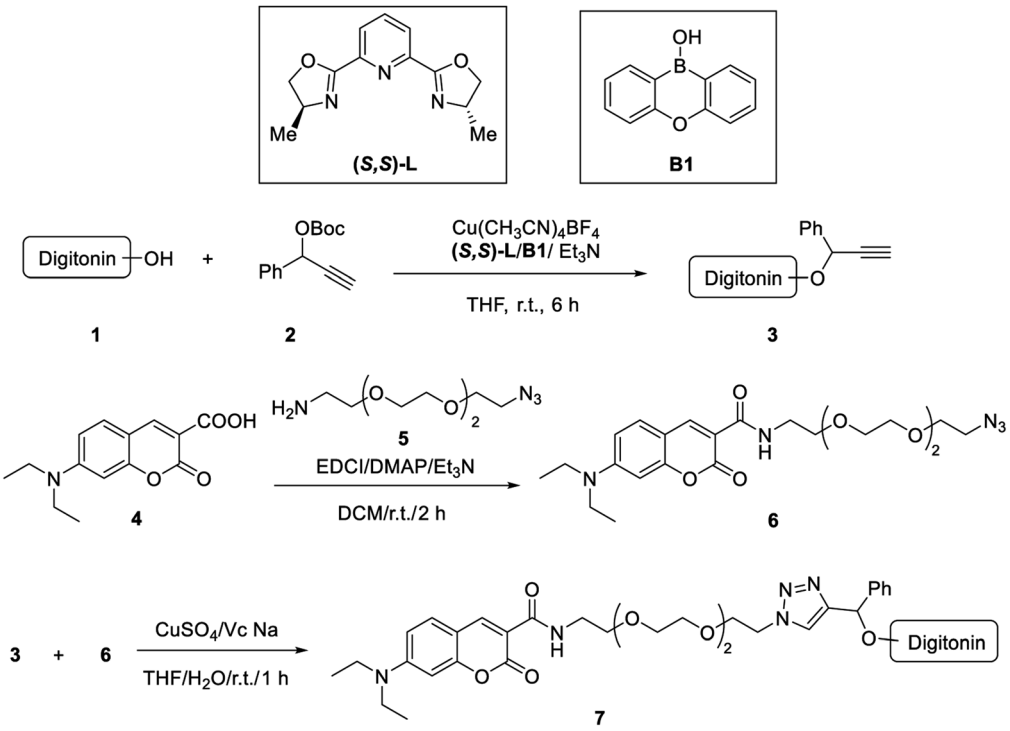

Scheme 2 Synthetic route and chemical structure of FDD.

the crude product and ultrasonicated for 20 min. After the solid was completely dispersed, a brown solid (compound **3**) was obtained by filtration.

Next, 7-(diethylamino) coumarin-3-carboxylic acid (compound **4**, 1300 mg, 5 mmol) and 11-azido-3,6,9-trioxaundecan-1-amine (compound **5**, 1200 mg, 5.5 mmol) were added slowly to *N*,*N*-dimethylformamide (50 mL) until dissolved, *N*-(3-dimethylaminopropyl)-*N*′-ethyl carbodiimide hydrochloride (1150 mg, 6 mmol), 1-hydroxybenzotriazole (811 mg, 6 mmol) and *N*,*N*-diisopropylethylamine (1940 mg, 15 mmol) were added and stirred overnight at room temperature. The complete consumption of **4** was monitored by thin-layer chromatography (TLC). The DMF was spin-dried with a rotary evaporator, 20 mL water was added, and the mixture was then extracted three times with 20 mL DCM. The organic layers were combined and washed with water (20 mL), saturated sodium bicarbonate (20 mL), and saturated brine (20 mL) in sequence. This was dried with anhydrous sodium sulphate and spin-dried with a rotary evaporator, followed by column chromatography (DCM : MeOH = 30 : 1) to obtain a brown oil (compound **6**).

Finally, to obtain our probe, compound **3** (450 mg, 0.15 mmol) and compound **6** (158 mg, 0.15 mmol) were dissolved in THF (3.5 mL), sodium ascorbate (VcNa, 68 mg, 0.15 mmol) and copper(II) sulphate (55 mg, 0.15 mmol, dissolved in 3.5 mL double distilled water) were added to the solution. The reaction mixture was stirred for 1 h at room temperature and the solvent was removed under reduced pressure, then 20 mL of THF was added and sonicated for 10 minutes. After filtering, the filtrate was spin-dried to obtain a brown solid, then 20 mL of solvent (petroleum ether/ethyl acetate, 10 : 1, v/v) was added to the crude product and ultrasonicated for 20 min. After the solid was completely dispersed, the brown solid (compound **7**) was obtained by filtration. To obtain the probe with higher quality, the resulting residue was purified twice by preparative high-performance liquid chromatography (prep-HPLC) to afford SCP as a light-yellow powder after freeze–drying. The optimal prep-HPLC conditions were obtained as follows. (1) Preparation conditions for the first separation, using a Waters Xbridge C18 preparation column (19 × 150 mm, 5 m), with 10 mmol bicarbonate amine – water (A) and acetonitrile (B) (volume ratio: 0 min, 50% A, 50% B; 1 min, 50% A, 50% B; 0.2 min, 50% A, 50% B; 8 min, 25% A, 75% B; 8.5 min, 5% A, 95% B; 10 min, 50% A, 50% B; 10.3 min, 50% A, 50% B; 13 min, 50% A, 50% B) as the mobile phase. Flow rate: 20 mL min^{-1}, loading amount: 100 mg and detection wavelength: 214 nm and 254 nm. (2) Preparation conditions for the second separation using a Waters Atlantis T3 preparation column (19 × 150 mm, 5 m), with 10 mmol ammonium acetate–water (A) and acetonitrile (B) (volume ratio: 0 min, 55% A, 45% B; 0.2 min, 55% A, 45% B; 8 min, 30% A, 70% B; 8.5 min, 5% A, 95% B; 10 min, 5% A, 95% B; 10.3 min, 55% A, 45% B; 13 min, 55% A, 45% B) as the mobile phase. Flow rate: 20 mL min^{-1}, loading amount: 100 mg and detection wavelength: 214 nm and 254 nm. FDD with a purity of 98.99% (214 nm) can be obtained from the above purification method (Fig. S1†). High-resolution mass spectral results confirmed that the measured molecular weight of FDD (1804.8544) was consistent with the theoretical value (1804.8541) (Fig. S2†).

FDD synthesised using the above method is a mixture, which is composed of a fluorescent group connected to the different hydroxyl groups of digitonin, but whichever hydroxyl group is

Open Access Article. Published on 22 June 2022. Downloaded on 1/13/2026 5:05:27 AM.
This article is licensed under a Creative Commons Attribution-NonCommercial 3.0 Unported Licence.

connected, it can be used for detecting skin cholesterol. Therefore, it is meaningless to characterise FDD by ^{1}H NMR and ^{13}C NMR. Several teams are trying to synthesize single compounds of these substances, but current technology does not guarantee the introduction of fluorophores on specific hydroxyl groups.[21–24] We hope that this method will be established as organic chemistry develops further. Although we could not characterize FDD by ^{1}H NMR and ^{13}C NMR, we separated and purified FDD by preparative high-performance liquid chromatography, and obtained FDD with a molecular weight of 1803.8 (one digitonin connected to one fluorescent group), and the measured purity was 98.99%. Furthermore, high-resolution mass spectral results confirmed that the measured molecular weight of FDD is consistent with the theoretical value. Therefore, these characterisations can ensure the consistency of the quality of the synthesised FDD from batch to batch.

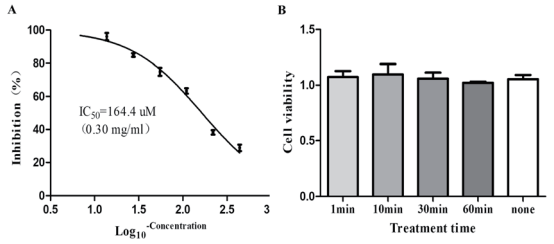

Fig. 1 Cytotoxic activities of FDD on the cell viability of human keratinocytes. (A) The inhibition of keratinocyte viability by FDD. Values (IC50) are the mean ± SD of triplicate experiments. (B) The viability of keratinocytes treated with 50 μM FDD for different times. Values are the mean ± SD of triplicate experiments.

2.2 The effect of FDD on the cell viability of human keratinocytes

Since FDD is used to detect the cholesterol content in the epidermis layer of the skin, we explored the toxicity of FDD on human keratinocytes. The concentration used for detecting skin cholesterol was 50 μM, we explored the effects of different concentrations of FDD on keratinocyte viability and obtained the IC_{50} value of 164.4 μM after incubation for 48 h. To further determine the effect of the used FDD concentration on the viability of keratinocytes, we treated the cells with 50 μM FDD for different times. The cell viability was determined 48 hours after changing the fresh medium and no major differences were seen in viability when the cells were treated with 50 μM FDD for different times (Fig. 1B). The results indicate that the use of 50 μM FDD is safe for the determination of cholesterol in the epidermis.

2.3 3-Dimensional fluorescence spectrum and fluorescence detection of FDD

The FDD was dissolved in DMSO at 10 mg mL^{-1}, and then diluted with pure water to the concentration of 50 μM, which was used for three-dimensional fluorescence spectral analysis, as shown in Fig. 2A. The excitation efficiency of the reagent was highest at about 250 nm and 405 nm; however, considering the damage of 250 nm light to human skin and eyes, we chose the 405 nm light source as the excitation source for the reagent. To evaluate the responsivity of FDD to cholesterol, 100 μL FDD (50 μM) was incubated with different contents of cholesterol fixed on a 96-well plate coated with chitosan. This amount of FDD

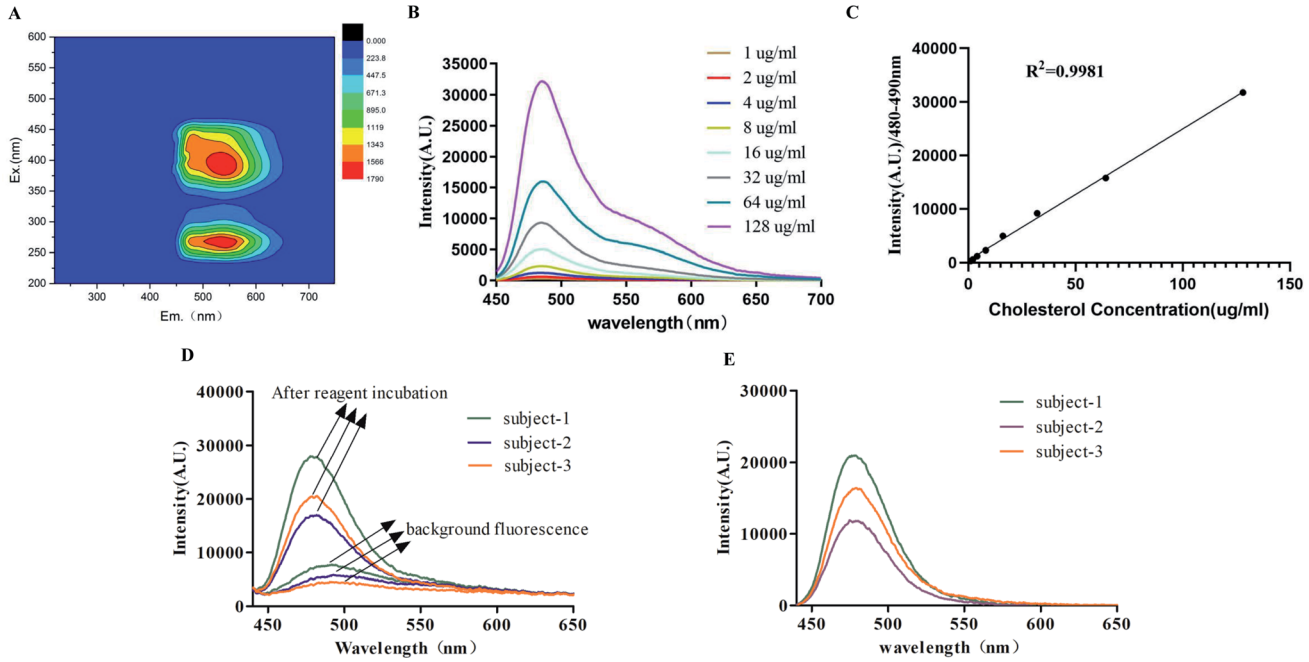

Fig. 2 Spectral properties of FDD. (A) The 3-dimensional fluorescence spectrum of FDD (50 μM). (B) Concentration-dependent fluorescence spectra of FDD (50 μM) towards cholesterol (1 μg mL^{-1}, 2 μg mL^{-1}, 4 μg mL^{-1}, 8 μg mL^{-1}, 16 μg mL^{-1}, 32 μg mL^{-1}, 64 μg mL^{-1}, 128 μg mL^{-1}). (C) The linearity of the fluorescence intensity (480–490 nm) *versus* different concentrations of cholesterol. (D) Fluorescence spectra of skin before and after incubation with 50 μM of FDD. (E) The fluorescence spectrum after subtracting the skin background fluorescence.

 © 2022 The Author(s). Published by the Royal Society of Chemistry

Open Access Article. Published on 22 June 2022. Downloaded on 1/13/2026 5:05:27 AM.
This article is licensed under a Creative Commons Attribution-NonCommercial 3.0 Unported Licence.

was sufficient to bind cholesterol in different wells. After blotting and washing with distilled water, the unbound FDD was washed away by blotting again, and the rest of the FDD is the FDD combined with different contents of cholesterol. As shown in Fig. 2B, there is a strong emission peak between 480 nm and 490 nm, which can be used as the characteristic emission spectrum of the FDD for detecting cholesterol. The average fluorescence intensity at 480–490 nm gradually increased with the increase in the cholesterol concentration. This result proves that the higher the cholesterol content, the more FDD is bound and the stronger the fluorescence intensity. Furthermore, a good linear correlation ($R^2 = 0.9981$) between the average fluorescence intensity at 480–490 nm and cholesterol concentration was found (Fig. 2C). These results suggest that the FDD can bind to different concentrations of cholesterol and the concentration of cholesterol can be analysed by the emission spectrum of the probe. Subsequently, we excited the skin with a 405 nm excitation light before incubating it with the FDD. The skin displays a background fluorescence that is generated by the excitation of intrinsic fluorescent substances in the skin (NADH, FAD, AGEs, *etc.*). After incubation with FDD, the excess FDD was washed with distilled water and removed by blotting. We stimulated the skin at the incubation site again with 405 nm excitation light, and we observed a strong fluorescence enhancement, which was the superposition of the skin background fluorescence and FDD fluorescence combined with cholesterol. When the skin background fluorescence is deducted, the remaining fluorescence is the fluorescence of FDD combined with cholesterol, and the cholesterol content can be deduced from the fluorescence intensity. As can be seen in Fig. 2D, there was a strong emission in the 450–550 nm band before and after the incubation. The fluorescence emission spectra after incubation showed a superposition of the skin background fluorescence and the FDD combined with the skin cholesterol. After subtracting the skin background fluorescence, the emission spectrum still showed a strong emission peak between 480 nm and 490 nm, which can also be used for the characteristic spectrum of FDD conjugated with different concentrations of cholesterol in the skin (Fig. 2E).

2.4 Selectivity and stability of FDD

To study the selectivity of FDD towards cholesterol, common lipids (cholesterol, fatty acid, ceramide 2 and ceramide 5) in the keratin of the skin were incubated with the 100 μL FDD in 96-well plates, after blotting and washing with distilled water, the unbound FDD was washed away by blotting again and their fluorescence intensities were recorded. As shown in Fig. 3, a significant fluorescence enhancement was observed in the presence of cholesterol. The fluorescence spectra displayed

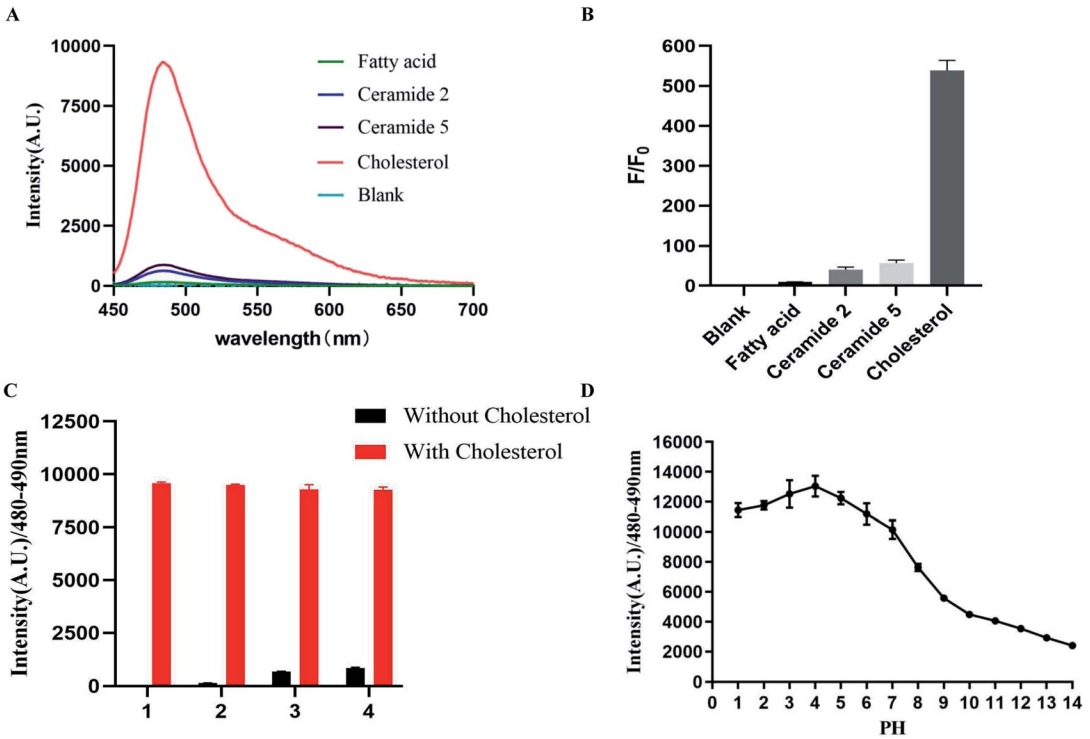

Fig. 3 The selectivity of FDD (50 μM). Fluorescence detection of cholesterol (32 μg mL^{-1}) using the FDD probe (50 μM) at 480–490 nm in the absence and presence of common lipid (1 mM) found in the keratin of the skin. (A) Fluorescence spectral changes in FDD (50 μM) for fatty acid, ceramide 2, ceramide 5 and cholesterol at RT. (B) Fluorescence ratio to blank (average fluorescence intensity at 480–490 nm) of FDD for common lipid in the keratin of the skin (lipids are cholesterol fatty acid, ceramide 2 and ceramide 5). (C) Black bars represent the average fluorescence intensity at 480–490 nm ($\lambda_{ex} = 405$ nm) of FDD in the presence of common lipid in the keratin of the skin (lipids are cholesterol, fatty acid, ceramide 2 and ceramide 5). The red bars represent the average fluorescence intensity at 480–490 nm that occurs in the presence of 32 μg mL^{-1} of cholesterol. (D) The effect of pH on the fluorescence intensity at 480–490 nm of FDD (50 μM).

Open Access Article. Published on 22 June 2022. Downloaded on 1/13/2026 5:05:27 AM.
This article is licensed under a Creative Commons Attribution-NonCommercial 3.0 Unported Licence.

almost no changes in the presence of fatty acid, however, there was a weak affinity between FDD and ceramide 2/ceramide 5 but the affinity between cholesterol and the FDD was 10 times that of ceramide (Fig. 3A and B). The competing experiment showed that other lipids could hardly interfere with the above detection process (Fig. 3C). These results confirmed that FDD exhibits high selectivity to cholesterol without obvious interference from other skin lipids. The effect of pH on the fluorescence intensity showed that the average fluorescence intensity (480–490 nm) can maintain a strong state at pH 3–7(Fig. 3D). The physiological pH of the stratum corneum is 4.1–5.8,[25] which indicates that FDD is stable in the skin detection environment.

2.5 Verification of the accuracy of skin cholesterol measurement

After determining the characteristic band of the skin cholesterol detection reagent, we used porcine skin and human skin tests to determine whether the fluorescence intensity of the characteristic band detected by the fluorescence reagent could reflect the cholesterol content of the skin. To mimic the measurement of skin cholesterol in different humans, porcine skin extracted with a mixture of ethanol and ethyl ether in a proportion of 3 : 1 for different time courses (0 min, 1 min, 2 min, 3 min, 4 min) was used to obtain the skin-containing gradient concentration of cholesterol. As shown in Fig. 4A and B, with the extension of the extraction time, the concentration of the skin cholesterol measured by gas chromatography gradually decreased, while the average fluorescence intensity in the 480–490 nm band detected by the reagent also decreased with the prolongation of the extraction time. This decrease is consistent with the decreasing trend detected by gas chromatography, indicating that the detection reagent can be used for the non-invasive detection of skin cholesterol.

In order to further clarify the accuracy of the reagent for detecting skin cholesterol, we used the detection reagent to detect the spectrum of cholesterol on the back skin of 46 experimental pigs and the hypothenar eminence area of the palms of 74 people, and then the cholesterol close to the measurement site was extracted with absolute ethanol for 2 minutes. The extract was measured by gas chromatography and the results showed that there was a significant correlation between the average fluorescence intensity and the gas chromatography measured value in both pig and human skin; the correlation coefficients were 0.9009 ($p < 0.0001$) and 0.8524 ($p < 0.0001$), respectively (Fig. 4C and E) The cholesterol content in pig skin is much higher than that in human skin, and these results indicated that the test reagent can detect skin tissue with a cholesterol content of 0–40 μg mL^{-1}. We have compared the mean fluorescence intensity detected by FDD with the values measured by gas chromatography using the Bland–Altman analysis. Fig. 4D shows that the Bland–Altman bias of pig skin was 7120 ± 1716 with 95% limits of agreement of 3757 to 10 482. The Bland-Altman bias of human skin was 2139 ± 760.8,

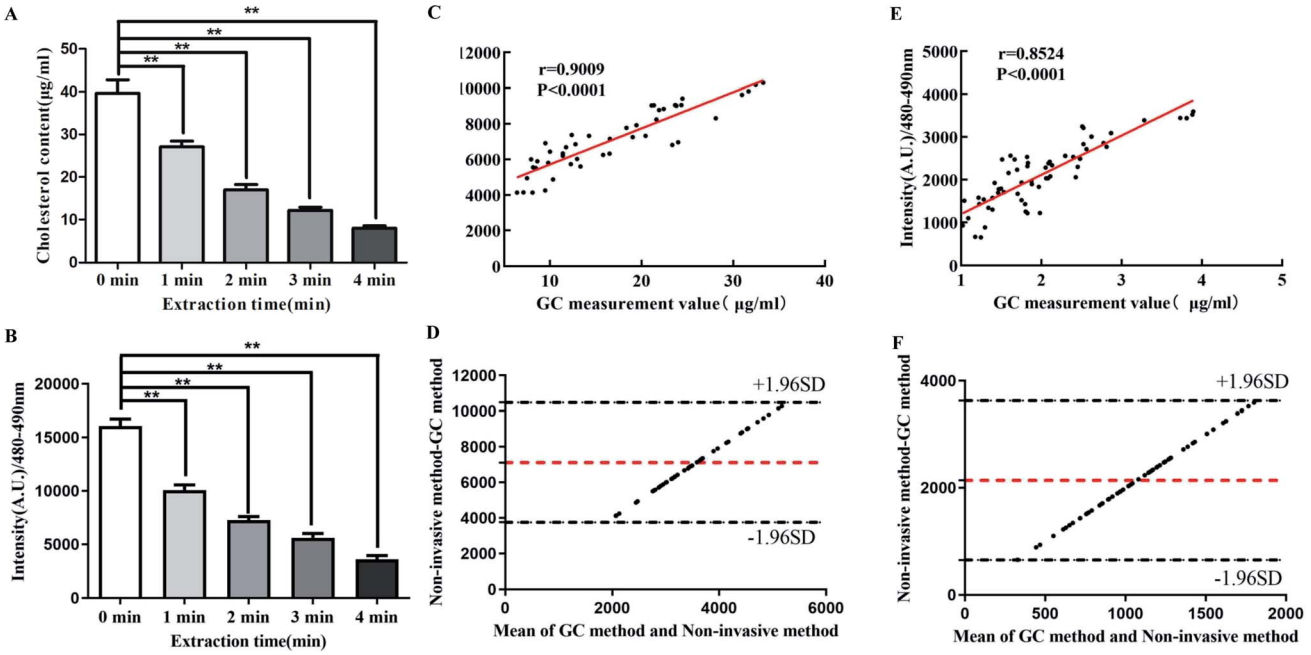

Fig. 4 Verification of the accuracy of FDD in measuring skin cholesterol. (A) Gas chromatography measured the concentration of cholesterol in porcine skin containing gradient concentrations of cholesterol obtained by extraction for different times. (B) The average fluorescence intensity (480–490 nm) of porcine skin containing gradient concentrations of cholesterol detected by FDD. (C) The correlation between skin cholesterol content measured by gas chromatography and the FDD detection method in porcine skin. (D) Bland–Altman analysis of the results detected by the FDD detection method and the values measured by gas chromatography in porcine skin. (E) The correlation between skin cholesterol content measured by gas chromatography and the FDD detection method in the hypothenar eminence area of the human palm. (F) Bland–Altman analysis of the results detected using the FDD detection method and the values measured by gas chromatography for the hypothenar eminence area of the human palm.

 © 2022 The Author(s). Published by the Royal Society of Chemistry

Open Access Article. Published on 22 June 2022. Downloaded on 1/13/2026 5:05:27 AM.
This article is licensed under a Creative Commons Attribution-NonCommercial 3.0 Unported Licence.

with 95% limits of agreement 647.5 to 3630 (Fig. 4F), falling within the prespecified clinically non-significant range. Both *in vivo* and *in vitro* results showed that the non-invasive method detected by FDD is a reliable and accurate method for the detection of skin cholesterol.

The best way to verify the accuracy is not to analyse the correlation between the FDD test results and the extracted skin cholesterol but after the FDD test is completed, remove the epidermal tissue in the detection area, and all the cholesterol in epidermal tissues should be measured, then compare the measured cholesterol and FDD test results. However, because this method requires a biopsy, few subjects are willing to perform the test. Next, we performed a series of algorithmic processing on the spectrum of each population to obtain more intuitive skin cholesterol measurements for clinical trials.

2.6 The detection reagent can distinguish between subclinical atherosclerosis, atherosclerosis patients and healthy individuals

To examine whether the detection reagent can recognize healthy individuals and atherosclerosis patients, as well as the high-risk atherosclerosis population, 135 atherosclerosis patients and 133 high-risk populations were measured; 133 low-risk individuals were also enrolled as normal groups. Detailed subject characteristics are shown in Table 1. The correlation analyses of other physiological parameters and skin cholesterol are shown in Table S1.† The results revealed that the disease group and high-risk groups had a significantly higher average fluorescence intensity at the 470–480 nm band compared to the normal group; however, the intensity between the disease group and high-risk group displayed no significant difference. The results revealed that the detection reagent can distinguish normal people from high-risk people or people with atherosclerosis diseases by detecting the content of skin cholesterol (Fig. 5A). The area under the ROC curve was applied to evaluate the efficacy of the mean fluorescence intensity in screening for atherosclerosis risk. As shown in Fig. 5B, the area under the ROC curve for distinguishing the normal/disease group was 0.9228 (95% confidence interval, 0.8938 to 0.9518), meanwhile, the area under the ROC curve for distinguishing the normal/risk group was 0.9422 (95% confidence interval, 0.9178 to 0.9665).

The fluorescence intensity of FDD bound to skin cholesterol in the high-risk group and disease group is significantly higher in the characteristic band than in the normal group. This result is consistent with our previous clinical data using enzymatic detection reagents.[11] Although the results show that there is a significant difference in skin cholesterol between the high-risk group and disease group, the fluorescence intensities of the characteristic band in the two groups are indistinguishable in most cases, this result suggests that skin cholesterol may not be suitable for distinguishing atherosclerosis patients from high-risk atherosclerosis. However, the skin cholesterol content of healthy individuals is significantly lower than that of the high-risk group and atherosclerosis patients. Therefore, skin cholesterol detected by FDD can be used as an indicator of risk screening for the atherosclerosis risk of normal people.

In order to ensure the accuracy of the research data, we conducted a strict selection of the research population. We performed a Framingham score on all the enrolled populations. People with scores below 10 are regarded as the normal group. Those with scores greater than 10 will be further subjected to angiography to determine the population with atherosclerotic disease. This is particularly important because the skin cholesterol content of the target population determined by angiography data can be obtained in this way. Detailed information on the subject exclusion criteria and clinical information collection and grouping is presented in the ESI.† We also analysed the associations between patient comorbidities with skin cholesterol, the results show that BMI, hypertension, blood glucose, HDL cholesterol (HDL-C) and triglycerides (TG) are not related to the skin cholesterol; only total cholesterol (TC) and LDL cholesterol (LDL-C) are weakly correlated with skin cholesterol content (Table 1 in ESI†). Our previous results and a study by Yashar *et al.* also indicated that skin cholesterol is not strongly associated with traditional risk factors.[11,26]

Our research has certain limitations. First, our study population was only the Chinese race, each group had only a few more than 100 samples, and the conclusions obtained do not

Table 1 Subject characteristics ($n = 401$)[a]

Variable	Normal group	Risk group	Disease group
N	133	133	135
Female (%)	52 (39.85%)	48 (36.09%)	45 (33.33%)
Age (years ± SD)	51.81 ± 11.23	53.42 ± 13.18	52.45 ± 13.17
BMI (kg m^{-2} ± SD)	25.99 ± 4.12	26.65 ± 4.78	26.33 ± 4.53
History of diabetes mellitus	10 (7.52%)	16 (12.03%)	17 (12.59%)
History of hypertension	36 (27.07%)	41 (30.83%)	43 (31.85%)
Current smoker	40 (30.08%)	47 (35.34%)	48 (35.56%)
Framingham score (%)	8.15 ± 2.17	17.12 ± 5.31**	19.68 ± 6.13**
TC (mmol L^{-1})	4.21 ± 0.52	5.47 ± 0.79*	5.48 ± 0.58*
LDL-C (mmol L^{-1})	3.13 ± 0.62	3.61 ± 0.82*	3.58 ± 0.66*
HDL-C (mmol L^{-1})	0.92 ± 0.18	0.91 ± 0.25	0.91 ± 0.28
TG (mmol L^{-1})	1.58 ± 0.41	1.60 ± 0.49	1.61 ± 0.37

[a] Continuous values are presented as mean ± SD. Categorical values are presented as the number of patients (percentage). *$P < 0.05$, **$P < 0.01$ *vs.* the normal group.

Open Access Article. Published on 22 June 2022. Downloaded on 1/13/2026 5:05:27 AM.
This article is licensed under a Creative Commons Attribution-NonCommercial 3.0 Unported Licence.

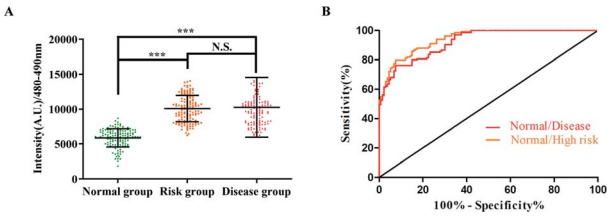

Fig. 5 FDD detection method can distinguish between subclinical atherosclerosis, atherosclerosis patients and healthy individuals. (A) Average fluorescence intensity (480–490 nm) of the normal group, disease group and high-risk group detected by the FDD method. (B) Receiver-operating characteristic (ROC) curves for distinguishing between the normal/disease group and normal/high-risk group.

apply to other races. Secondly, none of the participants involved in this study had undergone lipid-lowering treatment, so we do not know whether this method applies to the screening of the lipid-lowering treatment population. Finally, the mechanism by which the skin cholesterol content of people at a high risk of atherosclerosis and disease is significantly higher than that of normal people is not clear. Our multicentre clinical studies and prospective controlled trial are still going on. Further studies, informed by the work reported here, are needed to complete our understanding of the role of skin cholesterol in cardiovascular risk assessment from different races in different countries. It should also be determined whether various lipid-lowering treatments affect the content of skin cholesterol, which in turn affects the scope of application of FDD detection methods. The relationship between the formation of atherosclerosis in the arterial wall and the accumulation of skin cholesterol, and why skin cholesterol levels are associated with atherosclerosis should be clarified in the subsequent studies.

3. Conclusions

In this study, we synthesised a novel fluorescent digitonin derivative for non-invasive skin cholesterol detection. The FDD can be excited by a safe light source of 405 nm, and the emission wavelength band of 480 nm-490 nm can be used as the characteristic spectrum after combination with skin cholesterol. FDD displays many advantageous characteristics, such as low cytotoxicity, and high sensitivity to cholesterol without interference from other skin lipids. Promising results from the experiments have also shown the accuracy and reliability of this method. Meanwhile, clinical data suggest that healthy individuals and atherosclerosis patients, as well as the at-risk atherosclerosis population, can also be recognised by FDD. Therefore, this non-invasive method for skin cholesterol detection is a promising approach for atherosclerosis risk assessment and may potentially be used as a risk assessment tool for atherosclerosis screening in large populations.

4. Materials and methods

4.1 Keratinocytes cell viability assay

Cell viability was determined using the 3-(4,5-dimethylthiazol-2-yl)-2,5-diphenyltetrazolium bromide (MTT) assay. For the determination of the IC50, HaCat cells were grown in 96-well plates at a cell density of 2.5×10^4/well and treated with 6.875 μM (0.0125 mg mL^{-1}), 13.75 μM (0.025 mg mL^{-1}), 27.5 μM (0.05 mg mL^{-1}), 55.00 μM (0.1 mg mL^{-1}), 110.00 μM (0.2 mg mL^{-1}), 220 μM (0.4 mg mL^{-1}), 440 μM (0.8 mg mL^{-1}) of FDD for 48 h at 37 °C. The cells were incubated in the presence of MTT for 3 h at 37 °C. The absorbance was measured at 570 nm using a FLUOstar OPTIMA plate reader (BMG Labtech, Durham, NC, USA). To determine the effect of the FDD concentration on the viability of keratinocytes, the HaCat cells were grown in 96-well plates at a cell density of 2.5 × 104/well and treated with 50.00 μM (0.1 mg mL^{-1}) of FDD for different periods (1 min, 10 min, 30 min and 60 min). The cell viability was determined 48 hours after changing the fresh medium.

4.2 Obtaining porcine skin samples with different cholesterol contents

Skin samples were obtained from the abdomen of six Tibetan pigs weighing 30–35 kg, provided by the animal centre of Hefei Institutes of Physical Science, Chinese Academy of Sciences. After subcutaneous tissue was removed, the skin should soak in saline to exclude haemoglobin and other pollution. The skin was then dried in natural shade in the wake of cutting into rectangular shapes of 1.5 × 7.5 cm. Skin cholesterol was separated in a mixed solvent of ethanol and ethyl ether with a ratio of 3 : 1 for various times (0 min, 1 min, 2 min, 3 min and 4 min). The mixed solvent dissolves the cholesterol in the epidermis and with time, the cholesterol remaining in the epidermis becomes less and less. The skin contains various degrees of cholesterol that can be determined.

4.3 Participants

For this study, 401 members were enrolled successively from two locales, 266 people were recruited at the Health Management centre of First Affiliated Hospital of the University of Science and Technology of China, and 135 patients with clear vascular disease as indicated by angiogram were gathered from the department of cardiology of the First Affiliated Hospital of the University of Science and Technology of China. Everyone involved in the study had their skin cholesterol estimated and baseline risk data recorded, detailed information on exclusion criteria and grouping are given in the ESI.† Another 74 volunteers in the Health Management Centre were selected to partake in the accuracy confirmation. Everybody engaged in this investigation had their skin cholesterol measured with FDD, and then the detection site was extracted with 400 μL of absolute ethanol for 2 minutes. Cholesterol in the extractive fluid was detected right away with gas chromatography. Technicians at each site were trained indistinguishably to measure skin cholesterol. The study protocol was approved by the local ethics committee, and written informed consent was obtained from all patients.

4.4 Cholesterol measurement with gas chromatography

Cholesterol standards (Sigma-Aldrich) were dissolved in absolute ethanol at concentrations of 1 μg mL^{-1}, 2 μg mL^{-1}, 5 μg

 © 2022 The Author(s). Published by the Royal Society of Chemistry

Open Access Article. Published on 22 June 2022. Downloaded on 1/13/2026 5:05:27 AM. This article is licensed under a Creative Commons Attribution-NonCommercial 3.0 Unported Licence.

mL^{-1}, 10 μg mL^{-1}, 25 μg mL^{-1} and 50 μg mL^{-1}. Gas chromatography was used to detect the cholesterol content. The detection conditions of gas chromatography are as follows. Chromatographic column, DB-5 elastic quartz capillary column; carrier gas, high-purity nitrogen, purity ≥99.999%; constant flow rate, 2.4 mL min^{-1}; column temperature (programming temperature): the initial temperature was 200 °C, which was kept for 1 minute, increased to 280 °C at 30 °C min^{-1}, kept for 10 minutes; inlet temperature, 280 °C; detector temperature, 290 °C; injection volume: 1 μL; injection method: non-split injection, open the valve after injection for 1 minute; air flow rate: 350 mL min^{-1}; hydrogen flow rate: 30 mL min^{-1}. The cholesterol standard solution was injected into the gas chromatograph, and the peak area of the standard solution was measured under the above chromatographic conditions. The concentration was the abscissa and the peak area was the ordinate to prepare a standard curve. The extract was injected into a gas chromatograph to measure the peak area, and the concentration of cholesterol in the sample solution was obtained from the standard curve.

4.5 Three-dimensional fluorescence spectroscopy measurement

Three-dimensional fluorescence measurement of the detection reagent was performed on a Hitachi F-7000 spectrofluorometer equipped with a 150 W xenon lamp and connected to a PC microcomputer. The slit bandwidths of the excitation and emission monochromators were fixed at 5 nm. The voltage of the photomultiplier detector was set at 500 V and the scan rate at 12 000 nm min^{-1}. The excitation-emission fluorescence matrices were recorded with excitation wavelengths EX in the range of 200–600 nm and emission wavelengths EM 200–750 nm at a 4 nm interval.

4.6 Detection of the fluorescence spectrum of the reagent bound to skin cholesterol

The detailed detection steps are as follows. The Teflon gasket with detection well in the middle was attached to the small thenar part of the palm. Then, 100 μL of detection reagent was added to the detection well and after 1 min of incubation, the reagents were removed by blotting and 100 μL of distilled water was used to remove the excess reagent not bound to skin cholesterol. After an additional 30 s of cleaning, the washing fluid was removed by blotting, and the fluorescence spectrum of the reagent combined with skin cholesterol was measured using a self-built device.

4.7 General procedure for fluorescence measurement

Chitosan (2 g, Sigma-Aldrich, America) was dissolved in 2 mL of acetic acid, and 18 mL of pure water were added to obtain a 10% chitosan acetic acid aqueous solution, then diluted to 1% with pure water. 96-well plates were coated with 100 μL of 1% chitosan acetic acid in water at 37 °C for 2 h, then washed with pure water 3 times. Cholesterol was dissolved in absolute ethanol to obtain different concentrations of cholesterol solutions (1 μg mL^{-1}, 2 μg mL^{-1}, 4 μg mL^{-1}, 8 μg mL^{-1}, 16 μg mL^{-1}, 32 μg mL^{-1}, 64 μg mL^{-1}, 128 μg mL^{-1}). Solutions of other skin lipids were also prepared in absolute ethanol. The final concentration of the fatty acid (Merck, Germany), ceramide 2 (Merck, Germany) and ceramide 5 (Merck, Germany) was 1 mM. Here, 100 μL of each prepared solution was placed in a 96-well plate coated with chitosan, and 3 wells were repeated for each sample. After natural drying, each well of the 96-well plate can absorb different skin lipids. 100 μL FDD (50 μM) was incubated with the above-mentioned skin lipids in 96-well at RT for 1 min, the reagents were removed and excess unbonded reagents were rinsed with 100 μL pure water. After carefully removing the water with a pipette, the fluorescence spectrum was obtained with excitation at 405 nm and emission at 450–700 nm. We added 1.0 M HCl and 0.1 M NaOH to the 50 μM FDD to adjust the pH (1–14). The fluorescence intensity of FDD at different H was then measured using a fluorescence spectrophotometer (λ_{ex} = 405 nm). The area (S) of the band at 480–490 nm of the measured fluorescence spectrum was calculated, and then the average fluorescence intensity was calculated as $\frac{S}{490-480}$.

4.8 Statistical analysis

One-way analysis of variance (GraphPad, Prism 5) was used to compare multiple groups. The linear correlation analysis method was used to study the correlation between gas chromatography and the FDD measurement method in the determination of skin cholesterol content. The Bland–Altman analysis was used to compare and analyse the consistency of the FDD measurement method and gas chromatography. The area under the receiver operating characteristic curve was used to evaluate the diagnostic effect of the FDD detection methods. All analyses are expressed as mean ± SD, a P value < 0.05 is considered statistically significant.

Ethical statement

All animal experiments were performed duly in compliance with the guidelines set by the Anhui Committee of Use and Care of Laboratory Animals, and the overall project protocols were approved by the Animal Ethics Committee of Institutes of Physical Science, Chinese Academy of Sciences. All procedures performed in the studies involving human participates were in accordance with the 1964 Helsinkli declaration and its later amendments, and were approved by the ethics committee of the First Affiliated Hospital of University of Science and Technology of China. Informed consent was obtained from all individual participants included in the study.

Author contributions

All authors confirmed they have contributed to the intellectual content of this paper: Jingshu Ni: conceptualization, resources, validation, investigation, formal analysis, writing – original draft, visualization, writing – review & editing. Yong Liu: supervision, project administration, resources. Haiou Hong: methodology, investigation, formal analysis, validation. Xiangyong Kong: methodology, validation, formal analysis.

Open Access Article. Published on 22 June 2022. Downloaded on 1/13/2026 5:05:27 AM.
This article is licensed under a Creative Commons Attribution-NonCommercial 3.0 Unported Licence.

Yongsheng Han: methodology, validation, formal analysis. Lei Zhang: methodology, validation. Yang Zhang: investigation, validation. Yuanzhi Zhang: software, formal analysis, investigation. Changyi Hua: methodology, validation. Quanfu Wang: supervision. Xia Wang: project administration, supervision. Yao Huang: software, formal analysis. Meili Dong: supervision, writing – review, funding acquisition. Yikun Wang: supervision, project administration, writing – review, funding acquisition.

Conflicts of interest

The authors declare that they have no conflict of interest.

Acknowledgements

This work was funded by Science and Technology Major Project of Anhui Province of China (201903a07020027), Science and Technology Service Network Project, Chinese Academy of Sciences (KFJ-STS-QYZD-184), Natural Science Foundation of Anhui Province of China (1908085QH365), Key Research and Development Program of Anhui Province of China (202103a07020008, 202004a07020016 and 202104a07020023) and Key Project Supported by the President's Foundation of Hefei Institute of Physical Science, Chinese Academy of Sciences (YZJJZX202009). Support from the First Affiliated Hospital of University of Science and Technology of China is appreciated. The authors would also like to thank Anhui Provincial Institute for Food and Drug Control for their valuable opinions during the research period.

Notes and references

1 A. K. Dabrowska, F. Spano, S. Derler, C. Adlhart, N. D. Spencer and R. M. Rossi, *Skin Res. Technol.*, 2018, **24**, 165–174.
2 B. Dyring-Andersen, M. B. Lovendorf, F. Coscia, A. Santos, L. B. P. Moller, A. R. Colaco, L. Niu, M. Bzorek, S. Doll, J. L. Andersen, R. A. Clark, L. Skov, M. B. M. Teunissen and M. Mann, *Nat. Commun.*, 2020, **11**, 5587.
3 A. Kovacik, P. PuLlmannova, L. Pavlikova, J. Maixner and K. Vavrova, *Sci. Rep.*, 2020, **10**, 3832.
4 H. Yamamoto, M. Hattori, W. ChamuLitrat, Y. Ohno and A. Kihara, *Proc. Natl. Acad. Sci. U. S. A.*, 2020, **117**, 2914–2922.
5 I. K. Jung, J. Choi, J. Nam and K. T. No, *J. Cosmet. Dermatol.*, 2021, **20**, 2924–2931.
6 M. Sochorova, P. Audrlicka, M. Cervena, A. Kovacik, M. Kopecna, L. Opalka, P. PuLlmannova and K. Vavrova, *J. Colloid Interface Sci.*, 2019, **535**, 227–238.
7 H. Bouissou, M. T. Pieraggi, M. JuLian, I. Buscail, L. Douste-Blazy, E. Latorre and J. P. Charlet, *Atherosclerosis*, 1974, **19**, 449–458.
8 M. Girardet, B. Jacotot, F. Mendy, P. Piganeau and J. L. Beaumont, *J. Med.*, 1977, **8**, 261–278.
9 A. A. Melico-Silvestre, B. Jacotot, J. C. Buxtorf, V. Beaumont and J. L. Beaumont, *Pathol. Biol.*, 1981, **29**, 573–578.
10 R. Zawydiwski, D. L. Sprecher, M. J. Evelegh, P. Horsewood, C. Carte and M. Patterson, *Clin. Chem.*, 2001, **47**, 1302–1304.
11 J. Ni, H. Hong, Y. Zhang, S. Tang, Y. Han, Z. Fang, Y. Zhang, N. Zhou, Q. Wang, Y. Liu, Z. Li, Y. Wang and M. Dong, *Biomed. Eng.*, 2021, **20**, 52.
12 M. Reiter, S. Wirth, A. Pourazim, S. Puchner, M. Baghestanian, E. Minar and R. A. Bucek, *Vasc. Med.*, 2007, **12**, 129–134.
13 D. L. Sprecher and G. L. Pearce, *Am. Heart J.*, 2006, **152**, 694–696.
14 D. Vaidya, J. Ding, J. G. Hill, J. A. Lima, J. R. Crouse III, R. A. Kronmal, M. Szklo and P. Ouyang, *Atherosclerosis*, 2005, **181**, 167–173.
15 G. B. Mancini, S. Chan, J. Frohlich, L. Kuramoto, M. SchuLzer and D. Abbott, *Am. J. Cardiol.*, 2002, **89**, 1313–1316.
16 W. S. Tzou, M. E. Mays, C. E. Korcarz, S. E. Aeschlimann and J. H. Stein, *Am. Heart J.*, 2005, **150**, 1135–1139.
17 V. Raj, R. Jaime, D. Astruc and K. Sreenivasan, *Biosens. Bioelectron.*, 2011, **27**, 197–200.
18 H. Y. Fan and H. Heerklotz, *J. Colloid Interface Sci.*, 2017, **504**, 283–293.
19 K. Wojciechowski, M. Orczyk, T. Gutberlet, G. Brezesinski, T. Geue and P. Fontaine, *Langmuir*, 2016, **32**, 9064–9073.
20 B. Korchowiec, M. Janikowska-Sagan, K. Kwiecinska, A. Stachowicz-Kusnierz and J. Korchowiec, *J. Mol. Liq.*, 2021, 323.
21 W. Shang, B. He and D. Niu, *Carbohydr. Res.*, 2019, **474**, 16–33.
22 V. Dimakos and M. S. Taylor, *Chem. Rev.*, 2018, **118**, 11457–11517.
23 S. A. Blaszczyk, T. C. Homan and W. Tang, *Carbohydr. Res.*, 2019, **471**, 64–77.
24 G. Bati, J. X. He, K. B. Pal and X. W. Liu, *Chem. Soc. Rev.*, 2019, **48**, 4006–4018.
25 E. Proksch, *J. Dermatol.*, 2018, **45**, 1044–1052.
26 A. Y. Tashakkor and G. B. Mancini, *Can. J. Cardiol.*, 2013, **29**, 1477–1487.

 © 2022 The Author(s). Published by the Royal Society of Chemistry